J Petrol Explor Prod Technol (2015) 5:435–443
DOI 10.1007/s13202-014-0149-3

CrossMark

ORIGINAL PAPER - PRODUCTION ENGINEERING

Pressure transient and rate decline analysis for hydraulic fractured vertical wells with finite conductivity in shale gas reservoirs

Chaohua Guo · Jianchun Xu · Mingzhen Wei · Ruizhong Jiang

Received: 14 August 2014 / Accepted: 17 November 2014 / Published online: 2 December 2014

Abstract Producing gas from shale strata has become an increasingly important factor to secure energy over recent years for the considerable volume of natural gas stored. Unlike conventional gas reservoirs, gas transport in shale reservoirs is a complex process. In the organic nano pores, slippage effect, gas diffusion along the wall, viscous flow due to pressure gradient, and desorption from Kerogen coexist; while in the micro fractures, there exist viscous flow and slippage. Hydraulic fracturing is commonly used to enhance the recovery from these ultra-tight gas reservoirs. It is important to clearly understand the effect of known mechanisms on shale gas reservoir performance. This article presents the pressure transient analysis (PTA) and rate decline analysis (RDA) on the hydraulic fractured vertical wells with finite conductivity in shale gas reservoirs considering multiple flow mechanisms including desorption, diffusive flow, Darcy flow and stress sensitivity. The PTA and RDA models were established firstly. Then, the source function, Laplace transform, and the numerical discrete methods were employed to solve the mathematical model. At last the type curves were plotted and different flow regimes were identified. The sensitivity of adsorption coefficient, storage capacity ratio, interporosity flow coefficient, fracture conductivity, fracture skin factor, and stress sensitivity were analyzed. This work is important to understand the transient pressure and rate decline behaviors of hydraulic fractured vertical wells with finite conductivity in shale gas reservoirs.

Keywords Shale gas · Hydraulic fracturing · Pressure transient analysis · Rate decline analysis · Adsorption coefficient

List of symbols

C	Wellbore storage coefficient (m^3/Pa)
c_g	Gas compressibility (Pa^{-1})
C_f	Fracture conductivity
D	Diffusion coefficient (m^2/s)
h	Reservoir thickness (m)
k_{fh}	Horizontal permeability of natural fracture (m^2)
k_{fv}	Vertical permeability of natural fracture (m^2)
k_{fl}	Artificial fracture permeability (m^2)
$K_0()$	Modified Bessel function of second kind of order zero
L	Characteristic length (m)
L_{fLi}, L_{fRi}	Lengths of the left and right wings of the ith fracture (m)
n	Number of segments on the wing of each fracture
p_0	Reference pressure (Pa)
p_i	Initial reservoir pressure (Pa)
p_{sc}	Standard state pressure (Pa)
$\overline{q}$	Production rate from continuous point source (m^3/s)
$\overline{q}_i$	Flux per unit length of discrete segment (i, j), (m^2/s)
q_{sc}	Production rate (m^3/s)
r	Radial distance in natural fracture system (m)
R	External radius of matrix block (m)
S_f	Fracture skin factor, dimensionless

C. Guo (✉) · M. Wei
Department of Petroleum Engineering, Missouri University of Science and Technology, Rolla, MO 65401, USA
e-mail: Chaohua.Guo@mst.edu

J. Xu · R. Jiang
Department of Petroleum Engineering, China University of Petroleum (Huadong), Qingdao 266555, China

t	Time (s)
T	Reservoir temperature (K)
T_{sc}	Standard state temperature (K)
W_f	Fracture width (m)
u	Laplace transform parameter, dimensionless
V	Average volumetric gas concentration in the fracture (s-m^3/m^3)
V_E	Equilibrium volumetric gas concentration in pseudo-steady diffusion (s-m^3/m^3)
V_i	Initial volumetric gas concentration in the fracture (s-m^3/m^3)
x, y, z	Space coordinates in Cartesian coordinates (m)
xw, yw, zw	Space coordinates of continuous point source (m)
Z	Real gas compressibility factor, dimensionless
Z_i	Real gas compressibility factor under the initial condition, dimensionless
α	Adsorption index, dimensionless
λ	Inter-porosity flow coefficient, dimensionless
ω	Storativity ratio, dimensionless
τ	Sorption time constant (s)
ξ	Integration variable
μ	Gas viscosity (Pa s)
μ_i	Initial gas viscosity (Pa s)
φ_f	Natural fracture porosity, fraction
ψ	Pseudo-pressure (Pa)
ψ_i	Initial pseudo-pressure (Pa)

Superscript

_ Laplace domain

Subscripts

D Dimensionless
f Natural fracture
i Initial condition
m Matrix
sc Standard state
w Wellbore

Introduction

With the growing shortage of domestic and foreign energy industry, producing gas from shale gas reservoirs is currently received great attention due to their potential to supply the entire world with sufficient energy for the decades to come (Wang and Krupnick 2013). However, low gas recovery rate from unconventional shale resources remains the main technical difficulty. It is estimated that only 10–30 % of GIP can be recovered from these unconventional reservoirs. Most of the gas production wells can be low or no production capacity without hydraulic fracturing or horizontal well drilling. A shale gas reservoir is characterized as an organic-rich deposition with extremely low matrix permeability and clusters of mineral-filled "natural" fractures. Through core experiment analysis on 152 cores of nine reservoirs in North America, Javadpour found that the permeability of shale bedrock is mostly 54 nd (nano-Darcy) and about 90 % are less than 150 nd (Javadpour et al. 2007; Javadpour 2009). Most of the pore diameters are in the range of 4–200 nm (10^{-9} m). There are three forms for the gas to store in the shale: (1) free gas stored in the fractures and pores; (2) adsorption gas stored on the surface of the bedrock, in which Hill and Nelson estimated that 20–85 % of gas in shale is stored under this condition (Hill and Nelson 2000); (3) dissolved gas stored in the kerogen (Javadpour 2009).

Hydraulic fracturing has been used to create high conductivity flow path to improve the productivity of low permeability shale reservoirs (Waters et al. 2009; Rahm 2011; Arthur et al. 2009; Vermylen and Zoback 2011). Well test is an efficient method to understand gas flow mechanisms in unconventional shale and for better fracturing design (Prat 1990; Serra 1981; Bumb and McKee 1988; Brown et al. 2011; Bello and Wattenbarger 2010; Bello 2009). Bumb and McKee (1988) have considered the effect of desorption for shale gas well test. Brown et al. (2011) have studied PTA for fractured horizontal wells in unconventional shale reservoirs. Bello and Wattenbarger have studied RDA for multi-stage hydraulically fractured horizontal shale gas well (Bello and Wattenbarger 2010; Bello 2009).

However, there are few studies on well test and rate decline analysis for fractured vertical wells in shale gas reservoirs. Most of the research focused on the pressure response of infinite conductivity fractured wells in infinite formation (Standford 1974; Rosa and Carvalho 1989; Cinco-Ley and Samaniego 1981). So, it is necessary to study the pressure response for hydraulic fractured vertical wells, which is meaningful for effective shale gas production and deep understanding about gas flow mechanisms in unconventional shale reservoirs.

In this paper, based on shale gas flow mechanisms, such as desorption, diffusion, and flow in the fractures, the mathematical model which considers the effect of outer boundary effects for hydraulic fractured vertical wells with finite conductivity has been constructed. This model also considers Fick's first law of diffusion, Langmuir isothermal adsorption (Yin 1991), and stress sensitivity of natural fracture. Through point-source function method (Wei et al. 1999), the single-phase shale gas flow in matrix and fracture has been studied based on Fick's pseudo-steady state diffusion model (Cohen and Murray 1981). Sensitivity analysis has been carried out for significant factors, such as desorption constant, fracture conductivity coefficient,

storage capacity ratio, and inter-porosity flow coefficient. The effect of the above factors on the PTA and RDA has been presented.

Mathematical model

Assumptions

1. The shale gas formation consists of matrix system and fracture system. And there exists heterogeneity in the fracture system: the horizontal permeability and vertical permeability of the fracture system are different $k_{fh} \neq k_{fv}$;
2. Free shale gas exists in the fracture system and can be described using Darcy law;
3. Free gas and adsorption gas coexist in the matrix system;
4. The gas flow in the matrix system can be ignored. The gas in the matrix system first will desorb and then diffuse into the fracture system, which can be characterized using pseudo-steady state diffusion;
5. Single layer Langmuir isothermal curve can be used to describe the gas desorption from the matrix system;
6. Dynamic balance exists between adsorption gas and free gas;
7. The gas well is at constant production rate q_{sc} in standard condition;
8. The effect of gravity and capillary pressure can be ignored.

Mathematical model

Based on the above assumptions, combined with Darcy law, gas equation of state (EOS), and mass balance equation, the mathematical model can be established, which consists of desorption of shale gas, diffusion, and flow characteristics.

$$\frac{\partial}{\partial x}\left(k_{fh}\frac{p_f}{\mu Z}\frac{\partial p_f}{\partial x}\right)+\frac{\partial}{\partial y}\left(k_{fh}\frac{p_f}{\mu Z}\frac{\partial p_f}{\partial y}\right)+\frac{\partial}{\partial z}\left(k_{fv}\frac{p_f}{\mu Z}\frac{\partial p_f}{\partial z}\right)=\varphi_f c_{gf}\frac{p_f}{Z}\frac{\partial p_f}{\partial t}+\frac{p_{sc}}{T_{sc}}\frac{\partial V}{\partial t} \quad (1)$$

In the above Eq. (1), the second term in the right hand reflected the effect of the gas desorption.

The pseudo-pressure can be defined as follows:

$$\psi_f(p_f)=2\int_{p_0}^{p_f}\frac{p}{\mu Z}dp \quad (2)$$

Substitute Eqs. (2) into (1), we can obtain:

$$\frac{\partial}{\partial x}\left(k_{fh}\frac{\partial \psi_f}{\partial x}\right)+\frac{\partial}{\partial y}\left(k_{fh}\frac{\partial \psi_f}{\partial y}\right)+\frac{\partial}{\partial z}\left(k_{fv}\frac{\partial \psi_f}{\partial z}\right)=\varphi_f \mu_i c_{gfi}\frac{\partial \psi_f}{\partial t}+\frac{2p_{sc}T}{T_{sc}}\frac{\partial V}{\partial t} \quad (3)$$

According to Fick's first law of diffusion, if the matrix is assumed as sphere, the gas diffusion rate of shale matrix per unit time and per unit volume can be expressed as follows:

$$\frac{\partial V}{\partial t}=\frac{6D\pi^2}{R^2}[V_E(\psi_f)-V] \quad (4)$$

Also, we defined dimensionless variables as shown in Table 1.

The dimensionless forms for Eqs. (3) and (4) can be given as follows:

$$\frac{\partial^2 \psi_{fD}}{\partial x_D^2}+\frac{\partial^2 \psi_{fD}}{\partial y_D^2}+\frac{\partial^2 \psi_{fD}}{\partial z_D^2}=\omega\frac{\partial \psi_{fD}}{\partial t_D}-(1-\omega)\frac{\partial V_D}{\partial t_D} \quad (5)$$

$$\frac{\partial V_D}{\partial t_D}=\frac{V_{ED}(\psi_{fD})-V_D}{\lambda} \quad (6)$$

Taking Laplace transformation to t_D, Eqs. (5) and (6) become:

Then, Eqs. (5) and (6) can be changed to:

$$\frac{\partial^2 \overline{\psi}_{fD}}{\partial x_D^2}+\frac{\partial^2 \overline{\psi}_{fD}}{\partial y_D^2}+\frac{\partial^2 \overline{\psi}_{fD}}{\partial z_D^2}=\omega u\overline{\psi}_{fD}-(1-\omega)u\overline{V}_D \quad (7)$$

$$u\overline{V}_D=\frac{\overline{V}_{ED}(\psi_{fD})-\overline{V}_D}{\lambda} \quad (8)$$

Table 1 Definitions of the dimensionless variables

Dimensionless pseudo-pressure	$\psi_{fD}=\frac{\pi k_{fh}hT_{sc}}{p_{sc}q_{sc}T}(\psi_i-\psi_f)$
Dimensionless pseudo-time	$t_D=\frac{k_{fh}t}{\Lambda L^2}$
	$\Lambda=\varphi_f\mu_i c_{gfi}+\frac{2\pi k_{fh}h}{q_{sc}}$
Dimensionless coordinate	$x_D=\frac{x}{L}, y_D=\frac{y}{L}, z_D=\frac{z}{L}\sqrt{\frac{k_{fh}}{k_{fv}}}$
Dimensionless flow rate in the fracture system	$q_{fD}=\frac{2Lq_f(x_D,t_D)}{q_{sc}}$
Dimensionless gas concentration	$V_D=V-V_i$
Dimensionless storage capacity ratio	$\omega=\frac{\varphi_f\mu_i c_{gfi}}{\Lambda}$
Channeling coefficients	$\lambda=\frac{k_{fh}\tau}{\Lambda L^2}$
	$\tau=\frac{R^2}{6\pi^2 D}$
Dimensionless fracture width	$W_{fD}=\frac{W_f}{L}$
Dimensionless fracture conductivity	$C_{fD}=\frac{k_f W_f}{k_{fh}L}$
Adsorption coefficient	$\alpha=\frac{V_L p_L}{(p_L+p_f)(p_L+p_i)}\frac{p_{sc}q_{sc}T}{\pi k_{fh}hT_{sc}}\frac{\mu_i Z_i}{p_i}$
Dimensionless wellbore storage coefficient	$C_D=\frac{C}{2\pi h\Lambda L^2/\mu_i}$

According to Langmuir isotherm adsorption equation:

$$\overline{V}_{\mathrm{ED}}(\psi_{\mathrm{fD}}) = L[V_{\mathrm{E}} - V_{\mathrm{i}}] = L\left[\frac{V_{\mathrm{L}}p_{\mathrm{f}}}{p_{\mathrm{L}}+p_{\mathrm{f}}} - \frac{V_{\mathrm{L}}p_i}{p_{\mathrm{L}}+p_i}\right] \tag{9}$$

Taking Laplace transformation to t_D, Eq. (9) becomes:

$$\overline{V}_{\mathrm{ED}}(\psi_{\mathrm{fD}}) = -\frac{V_{\mathrm{L}}p_{\mathrm{L}}}{(p_{\mathrm{L}}+p_{\mathrm{f}})(p_{\mathrm{L}}+p_i)}\frac{p_{\mathrm{sc}}q_{\mathrm{sc}}T}{\pi k_{\mathrm{fh}}hT_{\mathrm{sc}}}\frac{\mu_i Z_i}{2p_i}\overline{\psi}_{\mathrm{fD}} \tag{10}$$

With the definition of Adsorption index in Table 1, we can get:

$$V_{\mathrm{ED}}(\psi_{\mathrm{fD}}) = -\alpha\psi_{\mathrm{fD}} \tag{11}$$

α is pseudo-pressure related, which can be assumed as a constant in the discussion range. And it is equal to the value in the initial reservoir state (Ertekin and Sung 1989; Anbarci and Ertekin 1990).

According to Eqs. (7), (8) and (11), we can obtain:

$$\frac{\partial^2\overline{\psi}_{\mathrm{fD}}}{\partial x_{\mathrm{D}}^2} + \frac{\partial^2\overline{\psi}_{\mathrm{fD}}}{\partial y_{\mathrm{D}}^2} + \frac{\partial^2\overline{\psi}_{\mathrm{fD}}}{\partial z_{\mathrm{D}}^2} = f(u)\overline{\psi}_{\mathrm{fD}} \tag{12}$$

$$f(u) = \omega u + \frac{\alpha u\lambda(1-\omega)}{u+\lambda} \tag{13}$$

Converting to spherical coordinates:

$$\frac{1}{r_{\mathrm{D}}^2}\frac{\partial}{\partial r_{\mathrm{D}}}\left(r_{\mathrm{D}}^2\frac{\partial\overline{\psi}_{\mathrm{fD}}}{\partial r_{\mathrm{D}}}\right) = f(u)\overline{\psi}_{\mathrm{fD}} \tag{14}$$

Inner boundary conditions:

$$\lim_{r_{\mathrm{D}}\to 0} r_{\mathrm{D}}\frac{\partial\overline{\psi}_{\mathrm{fD}}}{\partial r_{\mathrm{D}}} = -1 \tag{15}$$

Three forms of outer boundary conditions have been considered in this paper:

Infinite outer boundary (IOB):

$$\overline{\psi}_{\mathrm{fD}} = 0 \tag{16}$$

Constant pressure outer boundary (CPOB):

$$\psi_{\mathrm{fD}} = 0 \tag{17}$$

Closed outer boundary (COB):

$$\frac{\partial\psi_{\mathrm{fD}}}{\partial r_{\mathrm{D}}} = 0 \tag{18}$$

Apply the Laplace transform to both sides of the above equation from Eqs. (15)–(18). Then combining Eq. (14), we can obtain the line source solution under constant production rate condition:

$$\overline{\psi}_{\mathrm{f}} = \begin{cases} \dfrac{p_{\mathrm{sc}}T\tilde{q}}{T_{\mathrm{sc}}\pi k_{\mathrm{fh}}hu}\dfrac{1}{}K_0\left(r_{\mathrm{D}}\sqrt{f(u)}\right) & \text{IOB} \\ \dfrac{p_{\mathrm{sc}}T\tilde{q}}{T_{\mathrm{sc}}\pi k_{\mathrm{fh}}hu}\dfrac{1}{}\left[K_0\left(r_{\mathrm{D}}\sqrt{f(u)}\right) - \dfrac{K_0\left(r_{\mathrm{eD}}\sqrt{f(u)}\right)}{I_0\left(r_{\mathrm{eD}}\sqrt{f(u)}\right)}I_0\left(r_{\mathrm{D}}\sqrt{f(u)}\right)\right] & \text{CPOB} \\ \dfrac{p_{\mathrm{sc}}T\tilde{q}}{T_{\mathrm{sc}}\pi k_{\mathrm{fh}}hu}\dfrac{1}{}\left[K_0\left(r_{\mathrm{D}}\sqrt{f(u)}\right) + \dfrac{K_1\left(r_{\mathrm{eD}}\sqrt{f(u)}\right)}{I_1\left(r_{\mathrm{eD}}\sqrt{f(u)}\right)}I_0\left(r_{\mathrm{D}}\sqrt{f(u)}\right)\right] & \text{COB} \end{cases} \tag{19}$$

Solution

The schematic diagram of hydraulic fractured vertical well in shale gas reservoirs is shown in Fig. 1. There is one vertical well with finite conductivity after hydraulic fractured in a shale gas reservoir with top and bottom boundary closed. The well is produced at a constant rate q_{sc}. The reservoir pay zone is h. The hydraulic fracture totally fractured the whole reservoir, which means that the fracture height is h; The vertical cracks after hydraulic fracturing are symmetric against the wellbore. The fracture half length is x_{f} and fracture width is W_{f}. Fracture permeability is k_{f1}; Assume that the gas only flows into the wellbore through the hydraulic fractures. The fracture tips are closed with no gas flow.

Taking the case with IOB as an example, the pressure response can be obtained by superimposing line source solutions for shale gas reservoirs with top and bottom boundary closed:

$$\overline{\psi}_{\mathrm{fD}} = \frac{1}{2}\int_{-1}^{1}\overline{q}_{\mathrm{fD}}(u)K_0\left(\sqrt{(x_{\mathrm{D}}-\xi)^2+y_{\mathrm{D}}^2}\sqrt{f(u)}\right)d\xi \tag{20}$$

Here $\overline{q}_{\mathrm{fD}} = \frac{q_{\mathrm{fD}}}{u}$

Since the fracture is symmetric, following flow rate relationship can be obtained:

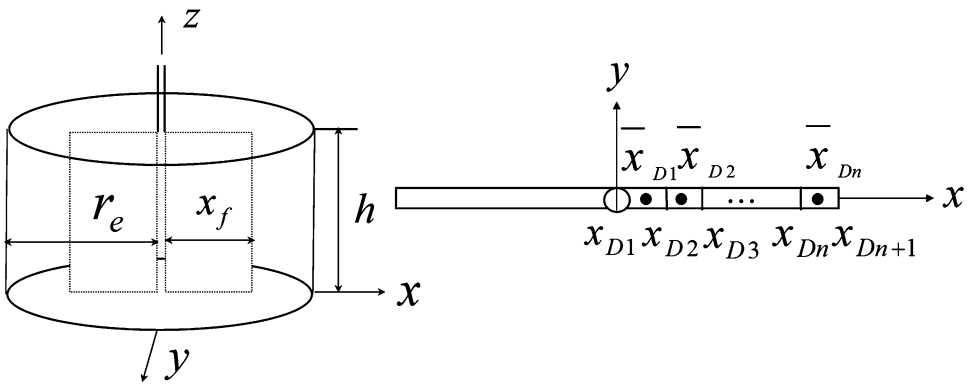

Fig. 1 Schematic diagram of hydraulic fractured vertical well. The *top* and *bottom* boundary are closed

$$\int_0^1 \overline{q}_{\mathrm{fD}} \mathrm{d}x_{\mathrm{D}} = \frac{1}{u} \tag{21}$$

Consider the skin effect by hydraulic fracturing, the fracture pseudo-pressure $\overline{\psi}_{\mathrm{fD}}$ can be related to formation pseudo-pressure $\overline{\psi}_{\mathrm{D}}$ using following equation:

$$\overline{\psi}_{\mathrm{fD}}(x_{\mathrm{D}}, u) = \overline{\psi}_{\mathrm{D}}(x_{\mathrm{D}}, y_{\mathrm{D}} = u) + \overline{q}_{\mathrm{fD}}(x_{\mathrm{D}}, u) \times S_{\mathrm{f}} \tag{22}$$

Ignoring the compressibility of fluids in the fracture, the following relationship can be obtained after combining boundary condition:

$$\overline{\psi}_{\mathrm{wD}} - \overline{\psi}_{\mathrm{f1D}}(x_{\mathrm{D}}, y_{\mathrm{D}} = 0, u) = \frac{\pi}{uC_{\mathrm{fD}}}\left[x_{\mathrm{D}} - u\int_0^{x_{\mathrm{D}}}\int_0^{\eta} \overline{q}_{\mathrm{fD}} \mathrm{d}x_{\mathrm{D}} \mathrm{d}\eta\right] \tag{23}$$

According to Eqs. (20) and (22), the above equation can be written in following form:

$$\begin{aligned}\overline{\psi}_{\mathrm{wD}} - \frac{1}{2}\int_0^1 \overline{q}_{\mathrm{fD}}(\xi, u)\Big[K_0\left(|x_{\mathrm{D}} + \xi|\sqrt{f(u)}\right) \\ + K_0\left(|x_{\mathrm{D}} - \xi|\sqrt{f(u)}\right)\Big]\mathrm{d}\xi - S_{\mathrm{f}} \times \overline{q}_{\mathrm{fD}} \\ + \frac{\pi}{C_{\mathrm{fD}}}\int_0^{x_{\mathrm{D}}}\int_0^{\eta} \overline{q}_{\mathrm{fD}} \mathrm{d}x_{\mathrm{D}} \mathrm{d}\eta = \frac{\pi}{uC_{\mathrm{fD}}} x_{\mathrm{D}}\end{aligned} \tag{24}$$

Equation (24) can be solved using discrete numerical methods. As shown in Fig. 1, the dimensionless fracture half length can be divided into n fractions with step length Δx_{D}. $\overline{x}_{\mathrm{D}i}$ is the center point of the ith discrete unit. $x_{\mathrm{D}i}$ is the end point of the ith discrete unit. As the discrete unit is small enough, the flow rate can be assumed to be uniformly distributed. Equation (24) can be discretilized into following form:

$$\begin{aligned}\overline{\psi}_{\mathrm{wD}} - \frac{1}{2}\sum_{i=1}^{n} \overline{q}_{\mathrm{fD}i}\int_{x_{\mathrm{D}i}}^{x_{\mathrm{D}i+1}} \Big[K_0\left(|\overline{x}_{\mathrm{D}j} + \xi|\sqrt{f(u)}\right) \\ + K_0\left(|\overline{x}_{\mathrm{D}j} - \xi|\sqrt{f(u)}\right)\Big]\mathrm{d}\xi - S_{\mathrm{f}} \times \overline{q}_{\mathrm{fD}j} \\ + \frac{\pi}{C_{\mathrm{fD}}}\left\{\sum_{i=1}^{j} \overline{q}_{\mathrm{fD}i}\left[0.5\Delta x_{\mathrm{D}}^2 + \Delta x_{\mathrm{D}}\left(\overline{x}_{\mathrm{D}j} - i\Delta x_{\mathrm{D}}\right) + \overline{q}_{\mathrm{fD}j}\frac{\Delta x_{\mathrm{D}}^2}{8}\right]\right\} = \frac{\pi}{uC_{\mathrm{fD}}} x_{\mathrm{D}}\end{aligned} \tag{25}$$

And the flow rate equation can be discretilized as follows:

$$\Delta x_{\mathrm{D}} \sum_{i=1}^{n} \overline{q}_{\mathrm{fD}i}(u) = \frac{1}{u} \tag{26}$$

There are $n + 1$ unknown variables in Eqs. (25) and (26), that is $\overline{\psi}_{\mathrm{wD}}$ and $\overline{q}_{\mathrm{fD}i}$(with $i = 1, 2, \ldots, n$). By solving these equations, in Laplace space, we can obtain the bottomhole pseudo-pressure $\overline{\psi}_{\mathrm{wD}}$ and the flow rate distribution in discrete units $\overline{q}_{\mathrm{fD}i}$.

Consider the effect of wellbore storage, according to Duhamel's principle, the bottomhole pressure response is

$$\overline{\psi}_{\mathrm{wD}} = \frac{\overline{\psi}_{\mathrm{wD}}}{1 + u^2 C_{\mathrm{D}} \overline{\psi}_{\mathrm{wD}}} \tag{27}$$

Using Stehfest inversion technique, we can obtain the bottomhole pseudo-pressure response in the real space.

Type curves and analysis

Type curves

Figure 2 is type curve for finite conductivity fractured vertical well in shale gas reservoirs with consideration of outer boundary effect in the log–log scale. The type curve can be divided into 8 stages: (1) the first stage is early afterflow period; the pseudo-pressure (PP) curve and pseudo-pressure-derivative (PPD) curve coincide with each other with the slope equal to 1; (2) the second stage is afterflow transition period; (3) the third stage is the bilinear flow period with slope of PPD curve equal to ¼; (4) the fourth stage is formation linear flow period with slope of PPD equal to ½; (5) the fifth stage is pseudo

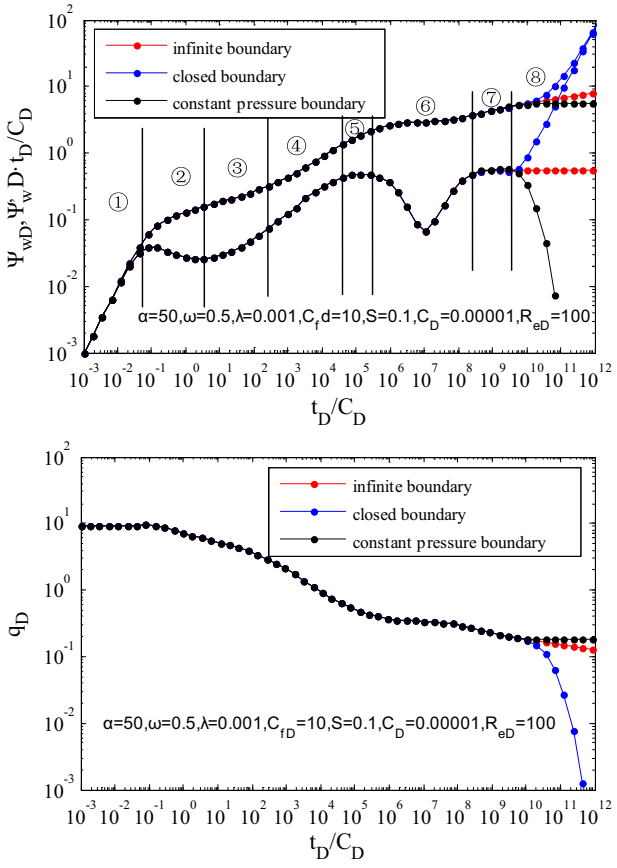

Fig. 2 Type curve for hydraulic fractured vertical wells with finite conductivity in shale gas reservoirs under different kinds of boundary conditions

radial flow of natural fractures with PPD equal to 0.5; (6) the sixth stage is the channeling period from matrix to fracture, and there is a concave in the PPD curve; (7) the seventh stage is the formation pseudo radial flow period with PPD equal to 0.5; (8) the eighth period is boundary response period. These scenarios will appear for different kinds of boundary conditions: PP curve and PPD curve will becomeupturned when the boundary is closed; otherwise, they will become downturned when the boundary is at constant pressure.

Sensitivity analysis

Effect of adsorption coefficient

Figure 3 shows the effect of adsorption coefficient on pseudo-pressure response (PPR) and rate decline response (RDR). Other parameters used are listed in the figure. From Fig. 3, it can be found that adsorption coefficient mainly affects the gas diffusion period from matrix to fracture. The larger the value, the concave in the PPD curve is wider and deeper. This suggested that the more gas desorbed, the more apparent is the diffusion. It can be also found that the larger the adsorption coefficient, the higher is the gas production rate. This suggests that the more gas desorbed, the more apparent is the diffusion. Also, from the definition of the adsorption coefficient, we know that the larger the Langmuir Volume, the larger is the adsorption coefficient, which also denotes the effect of the Langmuir volume.

Effect of storage capacity ratio

Figure 4 shows the effect of storage capacity ratio on PPR and RDR. Other parameters used are listed in the figure. From Fig. 4, we can find that storage capacity ratio not only affect the channeling period, but also has effect on transition period, linear flow period and formation linear flow period. The smaller the value, in the PPD curve, the wider and deeper are the concave. However, the position of PP and PPD curve in the transition period, linear flow period and formation linear flow period is more upper. Also, it can be found that the smaller the value, the smaller gas flow rate will be.

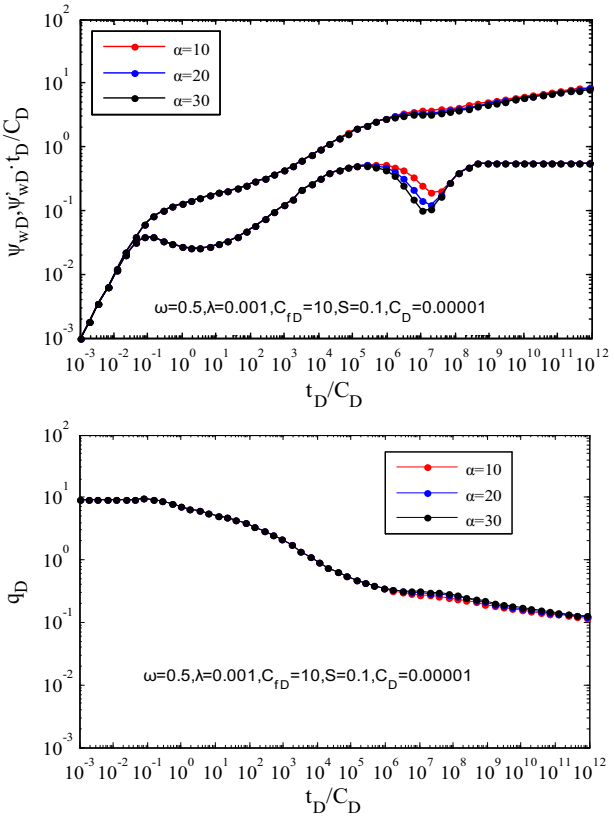

Fig. 3 Effect of adsorption coefficient on pseudo-pressure response (PPR) and rate decline response (RDR)

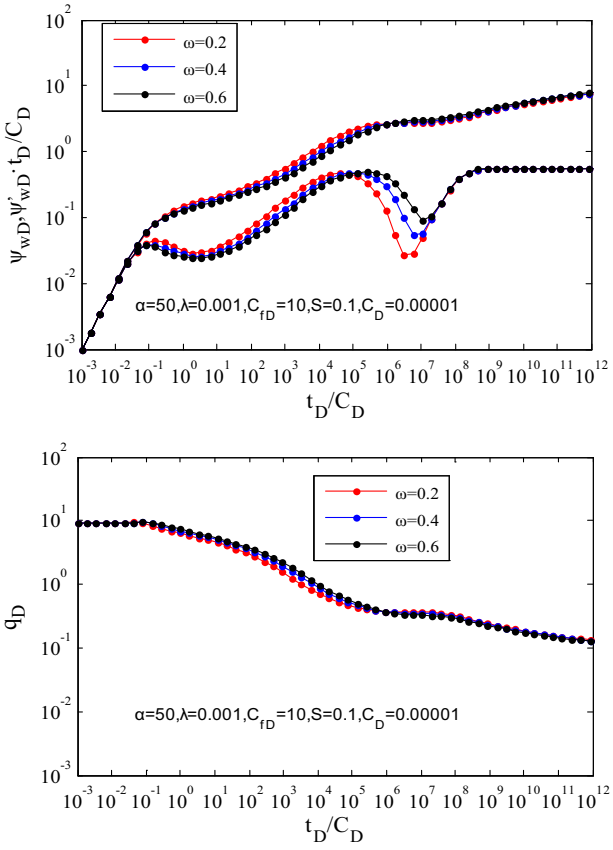

Fig. 4 Effect of storage capacity ratio on PPR and RDR

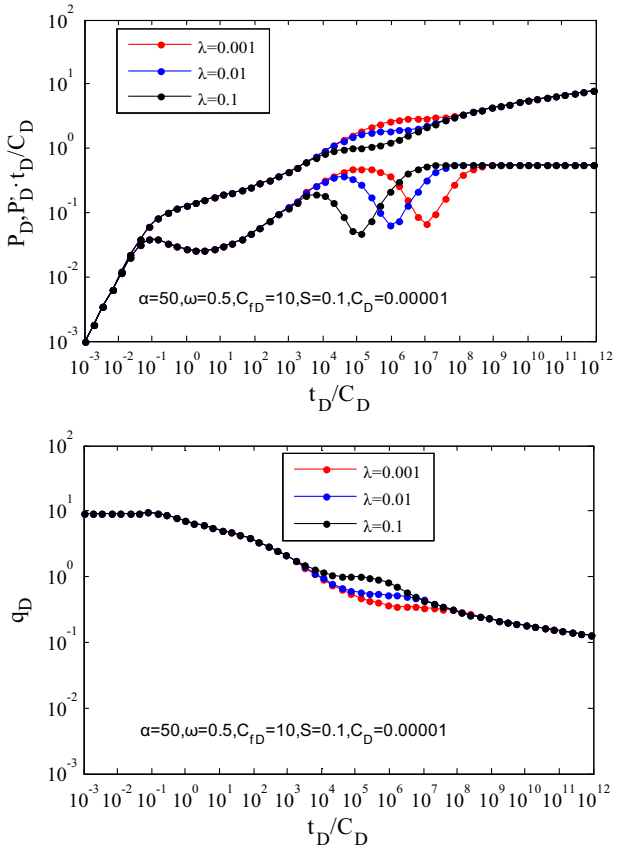

Fig. 5 Effect of channeling factor on PPR and RDR

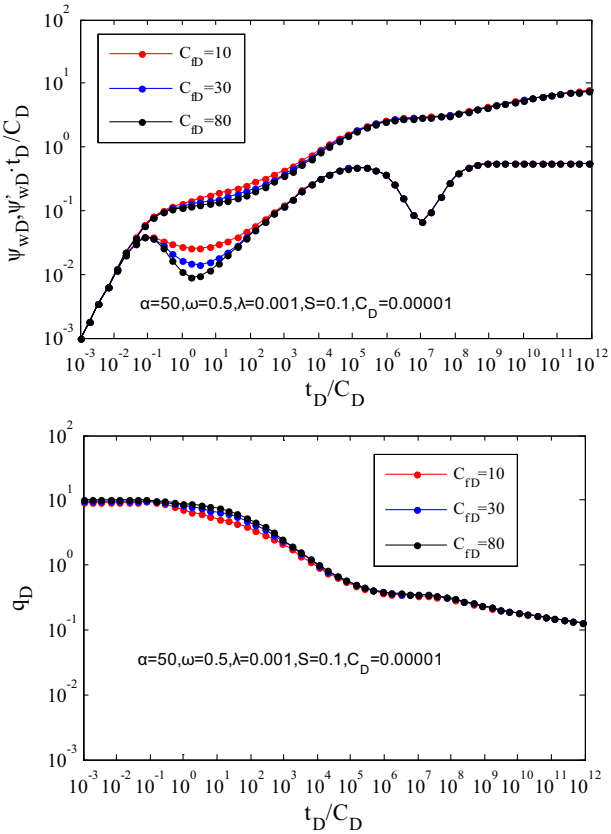

Fig. 6 Effect of fracture conductivity on PPR and RDR

Effect of channeling factor

Figure 5 shows the effect of channeling factor on PPR and RDR. Other parameters used are listed in the figure. From Fig. 5, we can find that channeling factor mainly affects the diffusion time from matrix to fracture. The larger the channeling factor, the earlier is the channeling start time, and the earlier is the appearance of the concave in the PPD curve. The larger the inter-porosity factor, the earlier is the matrix-fracture diffusion start time, and there will be a higher production rate.

Effect of fracture conductivity

Figure 6 shows the effect of fracture conductivity on PPR and RDR. Other parameters used are listed in the figure. From Fig. 6, we can find that the fracture conductivity mainly affects the transition period and early bilinear flow period. The larger the fracture conductivity, the characteristic of the early bilinear flow period is less clear. The PP and PPD curve are in lower position. When the value is larger enough, we cannot catch the early bilinear flow period. And the curve is close to the well-testing curve for infinite conductivity fractured well. Also, it can be found that the higher the fracture conductivity, the higher is the gas production rate.

Effect of fracture skin factor

Figure 7 shows the effect of fracture skin factor on PPR and RDR. Other parameters used are listed in the figure. From Fig. 7, we can find that the fracture skin factor mainly affects the flow from formation to fracture. The larger the value, the higher is the PP curve and more apparent is the hump effect. The larger the fracture skin factor, the more serious damage is during the hydraulic fracturing, and the lower the gas production rate is.

Effect of stress sensitivity

Figure 8 shows the effect of fracture stress sensitivity on PPR and RDR. Other parameters used are listed in the figure. From Fig. 8, we can find that the fracture stress sensitivity mainly affects the early period. The larger the value, the higher is the PP curve and the horizontal line of pressure curve is missing. And the larger the stress sensitivity, the higher is the production rate.

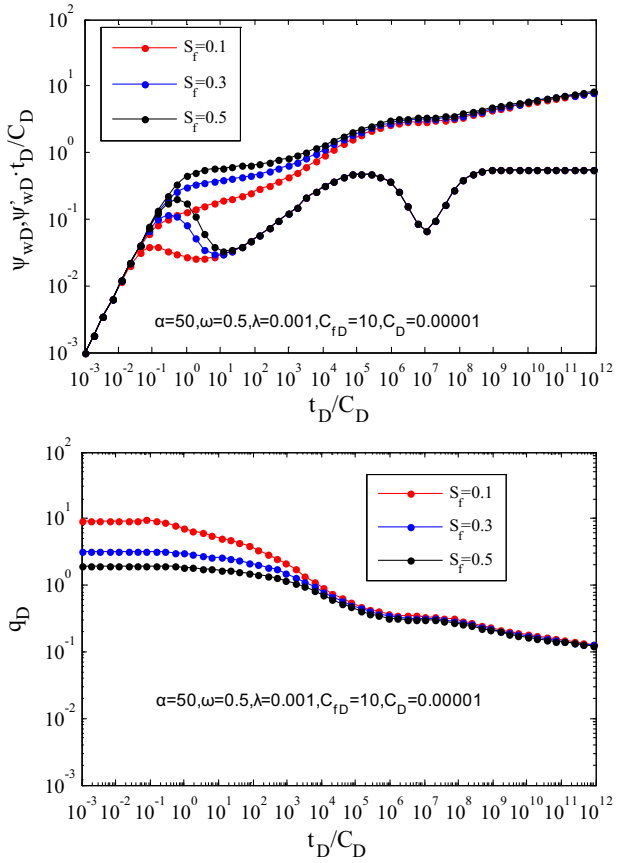

Fig. 7 Effect of fracture skin factor on PPR and RDR

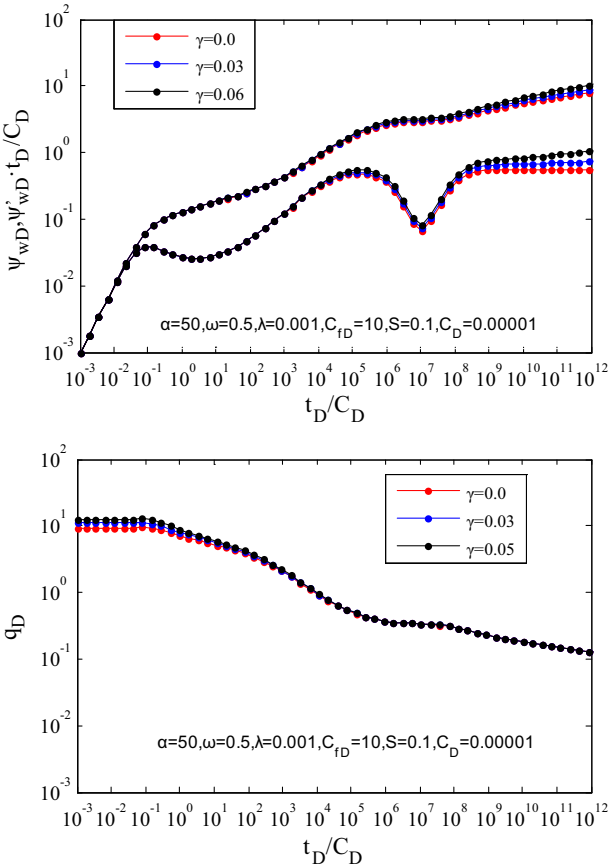

Fig. 8 Effect of stress sensitivity on PPR and RDR

Conclusions

In this paper, the pressure transient model and rate decline model for fractured vertical wells in shale gas reservoir have been presented, and the parameters' sensitivity analysis has been studied. The following conclusions can be summarized:

1. A mathematical model describing fluid flow of hydraulic fractured well in shale gas reservoirs is established and the solutions, transient pressure and rate decline curves are analyzed.
2. When the well is produced at a constant rate, a bigger Langmuir volume (V_L) will lead to a larger adsorption coefficient, which will cause a deeper depth of the trough during this period because big value of V_L indicates that more gas will be desorbed during the interporosity flow period.
3. The number of fractures (M_F) mainly affects the early flow regimes of the hydraulic fractured shale gas well, especially for the early linear and elliptical flow regimes. The more the M_F, the smaller are the pressure drop and the pressure decreasing rate.
4. When the well is produced at a constant bottom-hole pressure, the bigger the Langmuir volume (V_L) and well length, the greater the production rate will be in the later flow period.

Acknowledgments Funding for this project is provided by RPSEA through the "Ultra-Deepwater and Unconventional Natural Gas and Other Petroleum Resources" program authorized by the US Energy Policy Act of 2005. The authors also wish to acknowledge for the consultant support from Baker Hughes and Hess Company.

References

Anbarci K, Ertekin T (1990) A comprehensive study of pressure transient analysis with sorption phenomena for single-phase gas flow in coal seams. In: SPE Annual Technical Conference and Exhibition. Society of Petroleum Engineers

Arthur JD, Bohm B, Layne M (2009) Hydraulic fracturing considerations for natural gas wells of the Marcellus Shale.Gulf Coast Association of Geological Societies Transactions 59:49–59

Bello RO (2009) Rate transient analysis in shale gas reservoirs with transient linear behavior. Doctoral dissertation, Texas A&M University

Bello RO, Wattenbarger RA (2010) Multi-stage hydraulically fractured horizontal shale gas well rate transient analysis. In: North Africa Technical Conference and Exhibition. Society of Petroleum Engineers

Brown M, Ozkan E, Raghavan R, Kazemi H (2011) Practical solutions for pressure-transient responses of fractured horizontal wells in unconventional shale reservoirs. SPE Reserv Eval Eng 14(06):663–676

Bumb AC, McKee CR (1988) Gas-well testing in the presence of desorption for coalbed methane and devonian shale. SPE Form Eval 3(01):179–185

Cinco-Ley H, Samaniego FV (1981) Transient pressure analysis for fractured wells. J Petrol Technol 33(9):1749–1766

Cohen DS, Murray JD (1981) A generalized diffusion model for growth and dispersal in a population. J Math Biol 12(2):237–249

Ertekin T, Sung W (1989) Pressure transient analysis of coal seams in the presence of multi-mechanistic flow and sorption phenomena. SPE Gas Technology Symposium. Society of Petroleum Engineers

Hill DG, Nelson CR (2000) Gas productive fractured shales: an overview and update. Gas Tips 6(3):4–13

Javadpour F (2009) Nanopores and apparent permeability of gas flow in mudrocks (shales and siltstone). J Can Pet Technol 48(8):16–21

Javadpour F, Fisher D, Unsworth M (2007) Nanoscale gas flow in shale gas sediments. J Can Pet Technol 46(10):55–61

Prat G (1990) Well test analysis for fractured reservoir evaluation. Elsevier, Amsterdam

Rahm D (2011) Regulating hydraulic fracturing in shale gas plays: the case of Texas. Energy Policy 39(5):2974–2981

Rosa AJ, Carvalho RD (1989) A mathematical model for pressure evaluation in an lnfinite-conductivity horizontal well. SPE Form Eval 4(04):559–566

Serra K (1981) Well test analysis for devonian shale wells. University of Tulsa, Department of Petroleum Engineering, Tulsa

Standford U (1974) Unsteady-state pressure distributions created by a well with a single infinite-conductivity vertical fracture. Transactions of the American Institute of Mining, Metallurgical and Petroleum Engineers, p 257

Vermylen J, Zoback, MD (2011) Hydraulic fracturing microseismic magnitudes and stress evolution in the Barnett Shale Texas USA. In: SPE Hydraulic Fracturing Technology Conference. Society of Petroleum Engineers

Wang Z, Krupnick A (2013) A retrospective review of shale gas development in the United States. Resources for the Future Discussion Paper

Waters GA, Dean BK, Downie RC, Kerrihard KJ, Austbo L, McPherson B (2009) Simultaneous hydraulic fracturing of adjacent horizontal wells in the Woodford Shale. In: SPE Hydraulic Fracturing Technology Conference. Society of Petroleum Engineers

Wei G, Kirby JT, Sinha A (1999) Generation of waves in Boussinesq models using a source function method. Coast Eng 36(4):271–299

Yin Y (1991) Adsorption isotherm on fractally porous materials. Langmuir 7(2):216–217